Elucidation of phenotypic adaptations: Molecular analyses of dim-light vision proteins in vertebrates

Shozo Yokoyama*†, Takashi Tada*, Huan Zhang‡, and Lyle Britt§

*Department of Biology, Emory University, Atlanta, GA 30322; ‡Department of Marine Sciences, University of Connecticut, Groton, CT 06340; and §Alaska Fisheries Science Center, National Marine Fisheries Service, National Oceanic and Atmospheric Administration, Seattle, WA 98195

Edited by Masatoshi Nei, Pennsylvania State University, University Park, PA, and approved July 14, 2008 (received for review March 12, 2008)

Vertebrate ancestors appeared in a uniform, shallow water environment, but modern species flourish in highly variable niches. A striking array of phenotypes exhibited by contemporary animals is assumed to have evolved by accumulating a series of selectively advantageous mutations. However, the experimental test of such adaptive events at the molecular level is remarkably difficult. One testable phenotype, dim-light vision, is mediated by rhodopsins. Here, we engineered 11 ancestral rhodopsins and show that those in early ancestors absorbed light maximally (λ_{max}) at 500 nm, from which contemporary rhodopsins with variable λ_{max}s of 480–525 nm evolved on at least 18 separate occasions. These highly environment-specific adaptations seem to have occurred largely by amino acid replacements at 12 sites, and most of those at the remaining 191 (≈94%) sites have undergone neutral evolution. The comparison between these results and those inferred by commonly-used parsimony and Bayesian methods demonstrates that statistical tests of positive selection can be misleading without experimental support and that the molecular basis of spectral tuning in rhodopsins should be elucidated by mutagenesis analyses using ancestral pigments.

molecular adaptation | rhodopsin

The morphologies and lifestyles of animals in a wide range of environmental conditions have evolved to generate a striking array of forms and patterns. It is generally assumed that these variations have been driven by mutations, followed by positive Darwinian selection. However, it has been remarkably difficult not only to detect minute selective advantages caused by molecular changes (1), but also to find genetic systems in which evolutionary hypotheses can be tested experimentally (2). In the absence of proper experimental systems, molecular adaptation in higher eukaryotes has been inferred mostly by using statistical methods (for examples, see refs. 3–5). For several cases, however, ancestral molecules have been engineered, allowing studies of functional changes in the past (6). These analyses demonstrate that functional changes actually occurred, but they do not necessarily mean that the new characters were adaptive (7). To complicate the matter further, evolutionary changes are not always unidirectional and ancestral phenotypes may reappear during evolution (8, 9). One effective way of exploring the mechanisms of molecular adaptation is to engineer ancestral molecules at various stages of evolution and to recapitulate the changes in their phenotypes through time. To date, the molecular analyses of the origin and evolution of color vision produced arguably "the deepest body of knowledge linking differences in specific genes to differences in ecology and to the evolution of species" (10). The study of dim-light vision provides another opportunity to explore the adaptation of vertebrates to different environments.

Results

Rhodopsins. Dim-light vision in vertebrates is mediated by rhodopsins, which consist of a transmembrane protein, opsin, and a chromophore, 11-*cis*-retinal (11). By interacting with different opsins, the identical chromophores in different rhodopsins detect various wavelengths of light (reviewed in ref. 12). To explore the molecular basis of the spectral tuning in rhodopsins, *in vitro* assay-based mutagenesis experiments are necessary, in which the wavelengths of maximal absorption (λ_{max}s) can be measured in the dark (dark spectra) and/or by subtracting a spectrum measured after photobleaching from a spectrum evaluated before light exposure (difference spectra) (for example, see ref. 13). So far, the λ_{max}s of contemporary rhodopsins measured by using the *in vitro* assay vary between 482 and 505 nm (refs. 12 and 14 and references therein). By using another method, microspectrophotometry (MSP), the rhodopsin of a deep-sea fish, shining loosejaw (*Aristostomias scintillans*), has also been reported to have a λ_{max} of 526 nm (15).

To examine whether these λ_{max}s represent the actual variation of the λ_{max}s of rhodopsins in nature, we isolated the rhodopsins of migratory fish [Japanese eel (*Anguilla japonica*) and its close relative Japanese conger (*Conger myriaster*)], deep-sea fish [Pacific blackdragon (*Idiacanthus antrostomus*), Northern lampfish (*Stenobrachius leucopsarus*), shining loosejaw (*Aristostomias scintillans*), scabbardfish (*Lepidopus fitchi*), and Pacific viperfish (*Chauliodus macouni*)], and freshwater bluefin killifish (*Lucania goodei*), which live in diverse light environments (www.fishbase.org) [see supporting information (SI) *Methods* and Fig. S1]. The eel has two paralogous rhodopsins (EEL-A and -B), as do conger (CONGER-A and -B) and scabbardfish (SCABBARD-A and -B), whereas the others use one type of rhodopsins (BLACKDRAGON, LAMPFISH, LOOSEJAW, VIPERFISH and BFN KILLIFISH) (16) (see also *SI Result 1*).

In the *in vitro* assay, the λ_{max}s of the dark spectra are more reliable than those of difference spectra (*SI Result 2*) and, therefore, unless otherwise specified, the λ_{max}s refer to the former values throughout the paper. The λ_{max}s were determined for EEL-A (500 nm), EEL-B (479 nm), CONGER-A (486 nm), CONGER-B (485 nm), SCABBARD-A (507 nm), SCABBARD-B (481 nm), and BFN KILLIFISH (504 nm) (*SI Result 2*). The λ_{max}s for LAMPFISH and VIPERFISH could not be evaluated, but those of their difference spectra were 492 and 489 nm, respectively. Neither dark spectra nor difference spectra were obtained for BLACKDRAGON and LOOSEJAW. However, a mutant pigment, which is modeled after LOOSEJAW, has a difference spectrum λ_{max} of 526 nm (see *Molecular Basis*

Author contributions: S.Y. designed research; S.Y., T.T., H.Z., and L.B. performed research; S.Y. analyzed data; and S.Y. wrote the paper.

The authors declare no conflict of interest.

This article is a PNAS Direct Submission.

Data deposition: The sequences reported in this paper have been deposited in the GenBank database (accession nos. EU407248–EU407253).

See Commentary on page 13193.

†To whom correspondence should be addressed at: Department of Biology, Rollins Research Center, Emory University, 1510 Clifton Road, Atlanta, GA 30322. E-mail: syokoya@emory.edu.

This article contains supporting information online at www.pnas.org/cgi/content/full/0802426105/DCSupplemental.

of Spectral Tuning). Hence, the range of ≈480–525 nm seems to represent the λ_{max}s of rhodopsins in vertebrates reasonably well.

The Ecology of Dim-Light and Deep-Sea Vision. One of the critical times for the survival of animals in shallow water and on land is at twilight when the most abundant light falls between 400 and 500 nm (17). Many fish, amphibians, birds, and mammals that live in these environments use rhodopsins with λ_{max}s of ≈500 nm (12). In contrast, in deep water, the distribution of light is much narrower at ≈480 nm (18). Mature conger, mature eel, thornyhead, and coelacanth all live at the depths of 200–1,800 m (www.fishbase.org). Our data and that of others (19, 20) show that these fishes achieve their dim-light vision by using rhodopsins with λ_{max}s of ≈480 nm. Because of their λ_{max}s and specific light environments, the two groups of rhodopsins may be classified simply as "surface" and "deep-sea," respectively. Despite being active at much deeper depths of 3,000–4,000 m (www.fishbase.org), however, Northern lampfish and Pacific viperfish use rhodopsins with λ_{max}s of ≈490 nm. The higher λ_{max}s can be explained by their upward migration at night, and LAMPFISH and VIPERFISH can be regarded as "intermediate" rhodopsins. Then, through the use of far-red (≈700 nm) bioluminescence to create an artificial light environment, shining loosejaw achieves dim-light vision with the "red-shifted" rhodopsins (15).

Japanese eel spawns in the deep sea, the young adults migrate into freshwater, and the mature fish return to the deep sea for reproduction. Similarly, Japanese conger spawns in the deep sea, their larvae hatch near the coast, but they live only in the sea (www.fishbase.org). For their dim-light vision, young and adult eels use EEL-A and EEL-B, respectively, whereas congers use only CONGER-B; CONGER-A is expressed in the pineal complex (16). The λ_{max} of EEL-A (500 nm) reflects the shallow freshwater environment, whereas those of EEL-B and CONGER-B (480–485 nm) match with their light environments in the deep-sea. The λ_{max} of CONGER-A (486 nm) is similar to those of 470–482 nm in the pineal gland-specific pigments of American chameleon, pigeon, and chicken (reviewed in ref. 12). Hence, EEL-A is a surface rhodopsin and EEL-B and CONGER-B are deep-sea rhodopsins. CONGER-A does not reflect the deep-sea environment directly; however, because of its λ_{max}, CONGER-A may also be classified as a deep-sea rhodopsin.

Based on considerations of ecology, life history, and λ_{max}s of rhodopsins, dim-light vision can be classified into biologically meaningful deep-sea, intermediate, surface, and red-shifted vision (see *SI Result 3* for detailed discussion of the classifications of other rhodopsins). The corresponding rhodopsins have λ_{max}s of 479–486, 491–496, 500–507, and 526 nm, respectively, establishing the units of possible selection. Consequently, it is possible that selective force may be able to differentiate even 4–5 nm of λ_{max} differences of rhodopsins.

Ancestral Rhodopsins. Based on the composite phylogenetic tree (Fig. 1) (see also *SI Result 4* and Fig. S2) of the 11 newly characterized rhodopsins and 27 others from a wide range of vertebrate species, we inferred the amino acid sequences of ancestral rhodopsins. Because most of their rhodopsin genes have been sequenced partially (Fig. S3), squirrelfish (21) and cichlid (14) rhodopsins were first excluded from this inference. The amino acids inferred by using the Jones, Taylor, and Thornton and Dayhoff models of amino acid replacements of the PAML program (3) are highly reliable (*SI Results 5* and *6*, and Tables S1 and S2).

By introducing a total of 137 amino acid changes into various rhodopsins (Table S3), we then engineered pigments at nodes a–k (pigments a–k). The *in vitro* assays show that pigments a–d and f–h have λ_{max}s of 501–502 nm, whereas others have λ_{max}s of

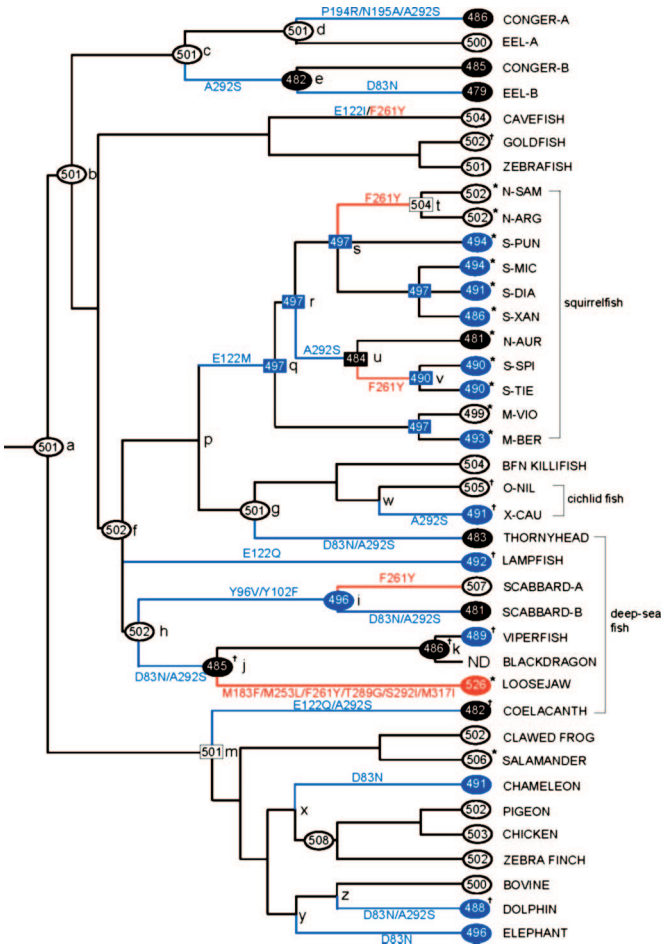

Fig. 1. A composite tree topology of 38 representative rhodopsins in vertebrates. Numbers in ovals are λ_{max}s evaluated from MSP (*), dark spectra, and difference spectra (†). The numbers in white, blue, black, and red ovals indicate surface, intermediate, deep-sea, and red-shifted rhodopsins, respectively, whereas those in rectangles indicate the expected values based on the mutagenesis results. Because of their incomplete data, the amino acid sequences of pigments a–k have been inferred by excluding the squirrelfish, bluefin killifish, and cichlid rhodopsins. S-PUN and S-XAN are classified as intermediate rhodopsins because of their expected λ_{max}s, but currently available data are ambiguous. Red- and blue-colored amino acid replacements indicate the color of the shifts in the λ_{max}. The λ_{max} of avian ancestral pigment shows that of the ancestral Archosaur rhodopsin (39). ND, the λ_{max} could not be determined.

496 nm (pigment i) and 482–486 nm (pigments e, j, and k), which are also highly reliable (*SI Results 5* and *6*).

Molecular Basis of Spectral Tuning. Because of the interactions between the 11-*cis*-retinal and various amino acids, the λ_{max} shifts caused by mutations in the opposite directions are often nonsymmetrical (22–24). Hence, to understand the evolutionary mechanism that has generated the various λ_{max}s of rhodopsins in nature, we must analyze "forward" amino acid replacements that actually took place in specific lineages. The reconstruction of multiple ancestral pigments opens an unprecedented opportunity to study the effects of such forward amino acid replacements on the λ_{max} shift in different lineages.

At present, certain amino acid changes at a total of 26 sites are known to have generated various λ_{max}s of rhodopsins and other paralogous visual pigments in vertebrates (25). The amino acid sequences of the 38 representative rhodopsins differ at 11 of the 26 sites (Fig. 2, second column). Among these, the specific amino

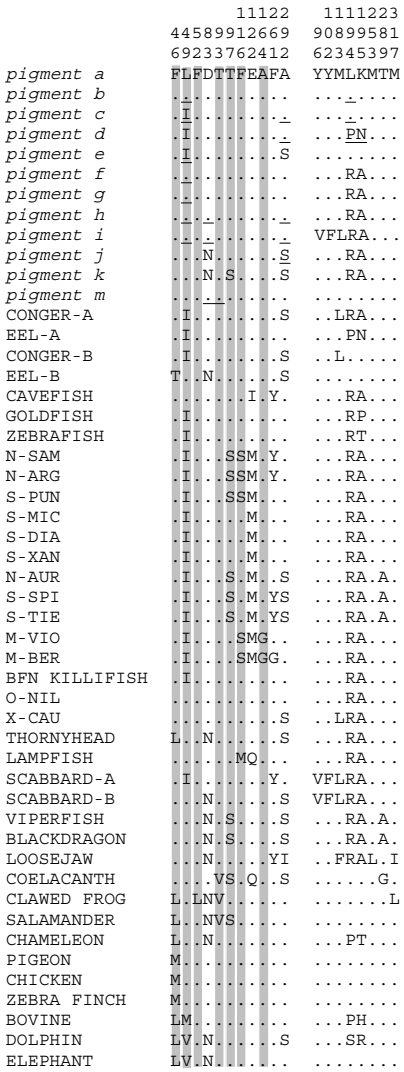

Fig. 2. Amino acids at the 11 previously known (25) and newly found critical residues of rhodopsins. The numerical column headings specify the amino acid positions, and the third column describes the newly discovered critical residues. Shades indicate amino acid replacements that are unlikely to cause any λ_{max} shifts (*SI Result 7*). Dots indicate the identity of the amino acids with those of pigment a. The ancestral amino acids that have a posterior probability of 95% or less are underlined.

acid replacements at 46, 49, 52, 93, 97, 116, and 164 are unlikely to have been involved in the spectral tuning (*SI Result 7*). These and other amino acid site numbers in this paper are standardized by those of the bovine rhodopsin (BOVINE). From the mutagenesis results (*SI Result 8* and Table S4), four key observations of evolutionary significance emerge.

First, the λ_{max}s of most contemporary rhodopsins can be explained largely by a total of 15 amino acid replacements at 12 sites. Namely, significant λ_{max} shifts have been caused by 4 of the 11 currently known sites (D83N, E122M, E122Q, F261Y, A292S, and S292I) as well as newly discovered sites Y96V, Y102F, E122I, M183F, P194R, N195A, M253L, T289G, and M317I (Fig. 2, third column). Therefore, the functional differentiation of vertebrate rhodopsin was caused mostly by only ≈3% of 354 amino acid sites.

Second, 4 of the 15 critical amino acid replacements occurred multiple times during rhodopsin evolution: D83N (seven times), A292S (nine times), F261Y (five times), E122Q (two times), and D83N/A292S (five times) (Fig. 1). Such extensive parallel changes strongly implicate the importance of these and other amino acid replacements at the 12 sites in the functional adaptation of vertebrate dim-light vision.

Third, we uncovered new types of amino acid interactions. A292S usually decreases the λ_{max} of rhodopsin by ≈10 nm (12) (see also pigments c and g in Table S4). Much to our surprise, when A292S was introduced into pigment d (Fig. 1), it did not decrease the λ_{max} at all. However, when the reverse mutation, S292A, was introduced into CONGER-A, a descendant of pigment d, the mutant rhodopsin increased the λ_{max} by 12 nm, explaining the λ_{max} of pigment d reasonably well. From the latter analysis alone, we may erroneously conclude that the λ_{max} of CONGER-A was achieved by A292S; instead, it was achieved purely by the interaction of three amino acid replacements (P194R, N195A, and A292S) (*SI Result 8*). Moreover, F261Y in pigment b increases the λ_{max} by 10 nm, and CAVEFISH, a descendant of pigment b, should have a λ_{max} of ≈510 nm, but the observed value is 504 nm (12), where the effect of F261Y was countered by E122I (for more details, see *SI Result 8*).

To study the molecular basis of spectral tuning, quantum chemists analyze the interactions between the 11-*cis*-retinal and amino acids that are located in the retinal binding pocket, within 4.5 Å of the 11-*cis*-retinal (26, 27). The residue 292 is ≈4.5 Å away from the 11-*cis*-retinal and is very close to the functionally critical hydrogen bonded network (28). However, the tertiary structure of the bovine rhodopsin (28) shows that the residues 194 and 195 are ≈20 Å away from residue 292 and are not even in the transmembrane segments. This magnitude of λ_{max} shift and the distance of interacting amino acids are totally unexpected.

The fourth significant observation is that the λ_{max} shifts of rhodopsins can be cyclic during vertebrate evolution. In particular, F261Y reversed the direction of λ_{max} shift four times (Fig. 1). If F261Y preceded E122I in the CAVEFISH lineage, then the functional reversions occurred five times.

Paleontology, Ecology, and Habitats. The ancestors of bony fish most likely used rhodopsins with λ_{max}s of ≈500 nm (Fig. 1). What types of light environment did these ancestors have? The origin of many early vertebrate ancestors is controversial, but that of bony fish ancestors is clear (29). The fossil records from late Cambrian and early Ordovician, ≈500 Mya, show that the ancestors of bony fish lived in shallow, near-shore marine environments (30–32). Therefore, pigment a must have functioned as a surface rhodopsin and its λ_{max} would be consistent with that role. Interpolating from the ancestral and contemporary rhodopsins, it is most likely that pigments b–d and f–h (λ_{max} = 501–502 nm) were also surface rhodopsins, pigment i (496 nm) was an intermediate rhodopsin, and pigments e, j, and k (480–485 nm) were deep-sea rhodopsins (Fig. 1). From their predicted λ_{max}s, it is also likely that pigments q, r, s, and v were intermediate rhodospins and pigment u was a deep-sea rhodopsin (Fig. 1).

Based on the four types of dim-light vision, vertebrates show six different evolutionary paths (Fig. 1). First, surface vision has been maintained in a wide range of species, from eels to mammals. Second, the transition of surface → intermediate vision also occurred in a wide range of species. Third, many deep-sea fish have achieved the directed transitions of surface → intermediate → deep-sea vision. The three additional changes are surface → intermediate → surface vision (some squirrelfish), surface → intermediate → deep-sea → intermediate vision (some squirrelfish and Pacific viperfish), and surface → intermediate → deep-sea → red-shifted vision (shining loosejaw), all showing that the evolution of dim-light vision is reversible.

Molecular Evolution. In vertebrate rhodopsins, several amino acid replacements occurred multiple times and, furthermore, the biologically significant λ_{max} shifts occurred on at least 18 sepa-

Table 1. Results from the NEB and BEB analyses

Rhodopsins	Model*	NEB	BEB
Squirrelfish	M2a	50 **162 213 214**	50 **162 213 214**
	M8	37 **50 162 213 214**	37 **50** 112 162 **213 214** 217
Squirrelfish and other fish	M2a	**162 212**	**162, 212**
	M8	**162, 212**	**162, 212**
Coelacanth and tetrapods	M2a	None	None
	M8	None	None
All	M2a	None	None
	M8	None	None

Sites with $P < 0.01$ levels are in bold.
*The null models and other parameters are given in Table S5.

rate occasions (Fig. 1). These observations strongly suggest that the 15 amino acid changes have undergone positive selection. To search for positively selected amino acid sites, we applied the naive-empirical-Bayes (NEB) and Bayes-empirical-Bayes (BEB) approaches of maximum-likelihood-based Bayesian method (3, 33) and parsimony method (4) to four sets of rhodopsin genes: (*i*) 11 squirrelfish genes; (*ii*) the squirrelfish rhodopsins and the bluefin killifish, cichlid, and deep-sea fish genes, excluding the coelacanth gene; (*iii*) the coelacanth and 9 tetrapod genes; and (*iv*) all 38 genes (Fig. 1).

Using the parsimony method, we could not find any positively selected amino acid sites. Using the Bayesian methods, however, a total of eight positively selected sites (positions 37, 50, 112, 162, 212, 213, 214, and 217) are predicted (Table 1). The Bayesian results reveal two characteristics. First, the positively selected amino acid sites are predicted only for relatively closely related genes, involving squirrelfish genes, but they disappear as more distantly related genes are considered together. It is also surprising that none of these predicted sites coincide with those detected by mutagenesis experiments. Second, different amino acids at these predicted sites do not seem to cause any λ_{max}-shifts (*SI Result 9*, Tables S5–S8, and Fig. S4).

Considering 17 closely related cichlid rhodopsin genes, 26 positively selected sites have also been predicted (34). Again, none of the different amino acids at these sites seem to cause any λ_{max} shifts and, furthermore, when we add the other 23 genes (the eel, conger, cavefish, goldfish, zebrafish, deep-sea fish, and tetrapod rhodopsin genes in Fig. 1) in the Bayesian analyses, all positively selected sites disappear (*SI Result 9*)! Why can positively selected sites be inferred more often in closely related genes than in distantly related genes? When nucleotide changes occur at random, the proportions of nonsynonymous and synonymous mutations are roughly 70% and 30%, respectively. Hence, under neutral evolution, or even under some purifying selection, closely related molecules can initially accumulate more nonsynonymous changes than synonymous changes. However, as the evolutionary time increases, synonymous mutations will accumulate more often than nonsynonymous mutations (35). The differential rates of synonymous and nonsynonymous nucleotide substitutions during evolution may explain the prediction of false-positives among the relatively closely related rhodopsins. Or, such inferences may also be affected by the statistical procedures (36).

As we saw earlier, D83N, Y96V, Y102F, E122I, E122M, E122Q, P194R, N195A, and A292S decreased the λ_{max}, whereas M183F, M253L, F261Y, T289G, S292I, and M317I increased it. These changes are located within or near the transmembrane segments, but most of the amino acid replacements at the remaining 191 neutral sites are scattered all over the rhodopsin molecule (Fig. 3).

Discussion

When moving into new dim-light environments, vertebrate ancestors adjusted their dim-light vision by modifying their rhodopsins. According to their λ_{max}s and light environments, rhodopsins are classified into four groups: deep-sea (≈480–485 nm), intermediate (≈490–495 nm), surface (≈500–507 nm), and red-shifted (≈525 nm) rhodopsins. Our mutagenesis results establish five fundamental features of molecular evolution that cannot be learned from the standard statistical analyses of protein sequence data.

First, mutagenesis experiments can offer critical and decisive tests of whether or not candidate amino acid changes actually cause any functional changes. Second, the same amino acid replacements do not always produce the same functional change but can be affected by the amino acid composition of the molecule. Therefore, the likelihood of parallel amino acid replacements, which may or may not result in any functional change, can overestimate the actual probability of functional adaptations (*SI Result 9*).

Third, similar functional changes can be achieved by different amino acid replacements; for example, D83N/A292S, P194R/N195A/A292S, and E122Q decrease the λ_{max} by 14–20 nm (Table S4). Thus, by simply looking for parallel replacements of specific amino acids, one can fail to discover other

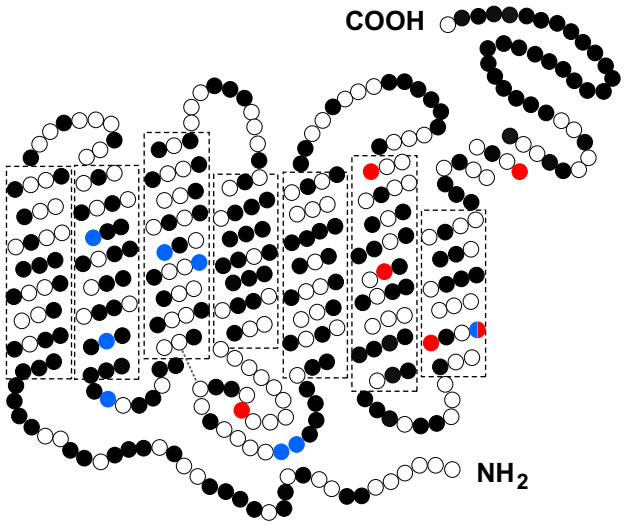

Fig. 3. Secondary structure of BOVINE (26) with a total of 203 naturally occurring amino acid replacements in the 38 vertebrate rhodopsins, where seven transmembrane helices are indicated by dotted rectangles. The amino acid changes that cause blue and red shifts in the λ_{max} are shown by blue and red circles, respectively, and those that are unlikely to cause any λ_{max} shifts are indicated by black circles.

amino acid replacements that generate the same functional change, thereby underestimating the chance of finding functional adaptations.

Fourth, not only can the identical mutations in different pigments cause different magnitudes of λ_{max} shift, but also mutations in the opposite directions often shift the λ_{max} to the opposite directions by different magnitudes. Hence, if we are interested in elucidating the evolutionary mechanisms of functional and phenotypic adaptations, we have to study forward mutations by using appropriate ancestral molecules rather than introducing mutations into contemporary molecules.

Fifth, even when the phylogenetic position of a molecule is unknown, its functional assay can clarify the molecular evolution of functional adaptation. For example, the phylogenetic position of LAMPFISH is uncertain (Fig. 1). However, because the E122Q that decreased the λ_{max} of pigment f is different from the other critical amino acid replacements in evolutionarily closely related rhodopsins, we can easily establish an independent origin of the functional change in LAMPFISH. To explore adaptive evolution of certain traits, therefore, both functional and molecular analyses of such traits are necessary.

Our analyses demonstrate that it is important to relate the functional changes of molecules to the ecological or behavioral changes that presumably caused the functional and phenotypic changes in the first place. Studying functional changes of ancestral rhodopsins and relating them to the associated environmental changes of organisms' habitats, we have established the mechanisms of functional adaptation of dim-light vision in vertebrates. To fully appreciate how adaptive evolution of dim-light vision has occurred, it is essential that the effects of critical amino acid changes on the λ_{max} shift are studied at the chemical level. Quantum chemical analyses of these amino acid changes will lead to a better understanding of the chemical basis of adaptive evolution of visual pigments and significantly enhance our understanding of the chemical basis of phototransduction in general.

Materials and Methods

Samples and Molecular Cloning of Rhodopsin Genes. High molecular weight DNAs of the five deep-sea fish (Northern lampfish, scabbardfish, Pacific viperfish, Pacific blackdragon, and shining loosejaw) were isolated from their body tissues by using a standard phenol-chloroform extraction procedure. The rhodopsin genes of these species were cloned by PCR and inverse PCR methods and were sequenced. The DNA sequences of the rhodopsin genes in Japanese eel (AJ249202, AJ249203), Japanese conger (AB043817, AB043818), and bluefin killifish (AY296738) were taken from GenBank.

Spectral Analyses of Rhodopsins. The contiguous intronless opsins were obtained by PCR amplification and expressed in COS1 cells, and the corresponding rhodopsins were regenerated by incubating the opsins with 11-*cis*-retinal. The absorption spectra of these rhodopsins were recorded by using a Hitachi U-3000 dual beam spectrophotometer (13).

Data Analyses. We considered 38 representative rhodopsins from 35 species: CONGER-A, CONGER-B (Japanese conger), EEL-A, EEL-B (Japanese eel), CAVEFISH (Mexican cavefish), GOLDFISH (goldfish), ZEBRAFISH (zebrafish), N-SAM, N-ARG, S-PUN, S-MIC, S-DIA, S-XAN, N-AUR, S-SPI, S-TIE, M-VIO, M-BER (squirrelfish), BFN KILLIFISH (bluefin killifish), O-NIL, X-CAU (cichlids), THORNYHEAD (thornyhead), LAMPFISH (Northern lampfish), SCABBARD-A, SCABBARD-B (scabbardfish), VIPERFISH (Pacific viperfish), BLACKDRAGON (Pacific blackdragon), LOOSEJAW (shining loosejaw), COELACANTH (coelacanth), CLAWED FROG (African clawed frog), SALAMANDER (tiger salamander), CHAMELEON (American chameleon), PIGEON (pigeon), CHICKEN (chicken), ZEBRA FINCH (zebra finch), BOVINE (bovine), DOLPHIN (bottlenose dolphin), and ELEPHANT (African elephant) (refs. 12, 14, 19, 21, 37, and 38 and references therein). Based on the phylogenetic-tree topology in Fig. 1, we inferred the amino acid sequences of ancestral pigments by using the PAML program(3). Positively selected amino acid sites of rhodopsins were inferred by using the maximum-likelihood-based Bayesian (3) and parsimony methods (4).

Genetic Engineering of Ancestral Pigments and Mutagenesis Analyses. The ancestral pigments were engineered by introducing a series of mutations into several contemporary rhodopsins (Table S3). All necessary mutations in reconstructing ancestral rhodopsins as well as forward and reverse mutations were introduced by using the QuikChange site-directed mutagenesis kit (Stratagene). To rule out spurious mutations, the DNA sequences of the mutant rhodopsins were sequenced.

ACKNOWLEDGMENTS. We thank P. Dunham, J. Lucchesi, M. Nei, Y. Tao, R. Yokoyama, and two anonymous reviewers for their helpful comments, B.G. Hall for his extensive editorial comments and many suggestions, N. Takenaka for her considerable technical contribution to this research, and R. Crouch for the 11-*cis*-retinal. This work was supported by the National Institutes of Health and Emory University.

1. Lewontin RC (1978) Adaptation. *Sci Amer* 239:3–13.
2. Yokoyama S (1977) Molecular genetic basis of adaptive selection: Examples from colour vision in vertebrates. *Annu Rev Genet* 31:315–336.
3. Yang Z (2007) PAML 4: A program package for phylogenetic analysis by maximum likelihood. *Mol Biol Evol* 24:1586–1591.
4. Suzuki Y, Gojobori T, Nei M (2001) ADAPTSITE: Detecting natural selection at single nucleotide sites. *Bioinformatics* 17:660–661.
5. Zhang J (2006) Parallel adaptive origins of digestive RNases in Asian and African leaf monkeys. *Nat Genet* 38:819–823.
6. Dean AM, Thornton JW (2007) Mechanistic approaches to the study of evolution: The functional synthesis. *Nat Rev Genet* 8:675–688.
7. Zhu G, Golding GB, Dean AM (2005) The selective cause of an ancient adaptation. *Science* 307:1279–1282.
8. Shi S, Yokoyama S (2003) Molecular analysis of the evolutionary significance of ultraviolet vision in vertebrates. *Proc Natl Acad Sci USA* 100:8308–8313.
9. Yokoyama S, Takenaka N (2004) The molecular basis of adaptive evolution of squirrelfish rhodopsins. *Mol Biol Evol* 21:2071–2078.
10. Carroll SB (2006) *The Making of The Fittest* (WW Norton & Co, New York).
11. Palczewski KG (2006) G protein-coupled receptor rhodopsin. *Annu Rev Biochem* 75:743–763.
12. Yokoyama S (2000) Molecular evolution of vertebrate visual pigments. *Prog Retin Eye Res* 19:385–419.
13. Yokoyama S (2000) Phylogenetic analysis and experimental approaches to study colour vision in vertebrates. *Methods Enzymol* 315:312–325.
14. Sugawara T, *et al.* (2005) Parallelism of amino acid changes at the RH1 affecting spectral sensitivity among deep-water cichlids from Lakes Tanganyika and Malawi. *Proc Natl Acad Sci USA* 102:5448–5453.
15. O'Day WT, Fernandez HR (1974) Aristomias scintillans (MALACOSTEIDAE): A deep-sea fish with visual pigments apparently adapted to its own bioluminescence. *Vision Res* 14:545–550.
16. Zhang H, *et al.* (2002) Isolation of freshwater and deep-sea type opsin genes from the common Japanese conger. *J Fish Biol* 61:313–324.
17. Muntz FW, McFarland WN (1977) in *Evolutionary Adaptations of Fishes to the Photic Environment*. Handbook of Sensory Physiology, ed Crescitelli F (Springer-Verlag, Berlin), vol VII/5, pp 193–274.
18. Jerlov NG (1976) *Marine Optics* (Elsevier, Amsterdam).
19. Yokoyama S, Tada T, Yamato T (2007) Modulation of the absorption maximum of rhodopsin by amino acids in the C-terminus. *Photochem Photobiol* 83:236–241.
20. Yokoyama S, Zhang H, Radlwimmer FB, Blow NS (1999) Adaptive evolution of color vision of the Comoran coelacanth (*Latimeria chalumnae*). *Proc Natl Acad Sci USA* 96:6279–6284.
21. Toller WW (1996) Rhodopsin evolution in the Holocentridae (Pisces: Beryciformes). PhD dissertation (University of Southern California, Los Angeles).
22. Asenjo AB, Rim J, Oprian DD (1994) Molecular determinants of human red/green color discrimination. *Neuron* 12:1131–1138.
23. Fasick JI, Lee N, Oprian DD (1999) Spectral tuning in the human blue cone pigment. *Biochemistry* 38:11593–11596.
24. Shi Y, Radlwimmer FB, Yokoyama S (2001) Molecular genetics and the evolution of ultraviolet vision in vertebrates. *Proc Natl Acad Sci USA* 20:11731–11736.
25. Yokoyama S, Takenaka N, Blow N (2007) A novel spectral tuning in the short wavelength-sensitive (SWS1 and SWS2) pigments of bluefin killifish (*Lucania goodei*). *Gene* 396:196–202.
26. Palczewski K, *et al.* (2000) Crystal structure of rhodopsin: A G protein-coupled receptor. *Science* 289:739–745.
27. Ebrey TG, Takahashi Y (2002) in *Photobiology for the 21st Century*, eds Coohill TP, Valenzeno DP (Valdenmar, Overland Park, KS), pp 101–133.
28. Okada T, *et al.* (2004) The retinal conformation and its environment in rhodopsin in light of a new 2.2Å crystal structure. *J Mol Biol* 342:571–583.
29. Carroll RL (1988) *Vertebrate Paleontology and Evolution* (WH Freeman & Co, New York).
30. Darby DG (1982) The early vertebrate *Astraspis*, habitat based on a lithologic association. *J Paleontol* 56:1187–1196.
31. Allulee JL, Holland SM (2005) The sequence stratigraphic and environmental context of primitive vertebrates: Harding sandstone, Upper Ordovician, Colorado, USA. *Palaios* 20:518–533.

32. Davies NS, Sansom IJ, Albanesi GL, Cespedes R (2007) Ichnology, paleoecology and taphonomy of a Gondwanan early vertebrate habitat: Insights from the Ordovician Anzaldo Formation, Bolivia. *Palaeogeogr*, *Palaeoclimatol*, *Palaeoecol* 249:18–35.
33. Yang Z, Wong WSW, Nielsen R (2005) Bayes empirical Bayes inference of amino acid sites under positive selection. *Mol Biol Evol* 22:1107–1118.
34. Spady TC, *et al*. (2005) Adaptive molecular evolution in the opsin genes of rapidly sepciating cichlid species. *Mol Biol Evol* 22:1412–1422.
35. Li W-H, Luo C-C, Wu C-I (1985) Evolution of DNA sequences. *Molecular Evolutionary Genetics*, ed MacIntyre RJ (Plenum Press, New York).
36. Suzuki Y, Nei M (2004) False-positive selection identified by ML-based methods: Examples from the Sig1 gene of the diatom Thalassiosira weissflogii and the tax gene of a human T-cell lymphotropic virus. *Mol Biol Evol* 21:914–921.
37. Chinen A, Hamaoka T, Yamada Y, Kawamura S (2003) Gene duplication and spectral diversification of cone visual pigments of zebrafish. *Genetics* 163:663–675.
38. Yokoyama S, Takenaka N, Agnew DW, Shoshani J (2005) Elephant and human color-blind deuteranopes have identical sets of visual pigments. *Genetics* 170:335–344.
39. Chang BSW, Jonsson K, Kazmi MA, Donoghue MJ, Sakmar TP (2002) Recreating a functional ancestral Archosaur visual pigment. *Mol Biol Evol* 19:1483–1489.